NASA Technical Memorandum 104416

A Comparison of Fiber Effects on Polymer Matrix Composite Oxidation

Kenneth J. Bowles
Lewis Research Center
Cleveland, Ohio

Prepared for the
Second Japan International Symposium and Exhibition
sponsored by the Society for the Advancement of
Materials and Process Engineering
Chiba, Japan, December 11-14, 1991

NASA

A COMPARISON OF FIBER EFFECTS ON POLYMER MATRIX COMPOSITE OXIDATION

Kenneth J. Bowles
National Aeronautics and Space Administration
Lewis Research Center
Cleveland, Ohio 44135

ABSTRACT

A number of thermo-oxidative stability studies addressing the effects of fiber reinforcement on composite thermal stability and the influence of geometry on the results of aging studies have been performed at the Lewis Research Center. The information presented herein, a compilation of some results from these studies, shows the influence of the reinforcement fibers on the oxidative degradation of various PMR-15 composites. Reinforcement of graphite and ceramics were studied and three composite oxidation mechanisms were observed. One was a dominant attack of the reinforcement fiber, the second was the aggressive oxidation of the matrix material, and the third was interfacial degradation.

KEYWORDS:

E-6248

1. INTRODUCTION

A number of studies have been conducted to investigate the thermo-oxidative behavior of polymer matrix composites (1-6). Two significant observations have been made as a result of these research efforts. The first is that the fiber reinforcement has a significant effect on the composite thermal stability (1-5), and the second is that there are geometric effects which have to be taken into consideration in evaluating thermal aging data (4-7).

At the time this series of studies was conducted, it appeared that Celion 6000 graphite fiber would be a standard reinforcement for high temperature polyamide composites because of the excellent mechanical properties it imparts to the composites. As time progressed, graphite fibers more thermally stable than the Celion 6000 reinforcement were made available.The consensus was that these fibers should produce a more thermally stable composite than the control and therefore could be considered for future use in high temperature structures. As a result of this thinking, the thermally stable T40-R fibers, along with some very stable ceramic fibers were

selected for high temperature air aging studies in PMR-15 composites. Nicalon (silicon carbide) and Nextel 321 (Aluminum oxide-silica-boron oxide) were the ceramic fibers that were selected.

A number of polymer matrix composite thermo-oxidative stability studies that address these areas have been carried out at the Lewis Research Center (1,4-6). The information presented herein is a compilation of some of the results of these studies which show the influence of the reinforcement fibers on the oxidative degradation and mechanical behavior of various polymer matrix composites.

2. MATERIALS

Only one matrix, the polyamide PMR-15, was used in these studies. The formulation of the monomers and the processing of the composites are adequately described elsewhere (8). All the laminates that were studied were unidirectional composites made from prepreg tape. The control material was reinforced with Celion 6000 graphite fiber. Except for the Nextel 312 fiber and some Nicalon fibers, all the fibers that were studied were unsized. The Nextel fiber was sized with A-1100 sizing (silane sizing). The Nicalon fiber was received in two batches. The first batch was sized with polyvinyl acetate (PVA). Some composites were processed with this sized fiber and some composites were processed with fibers that had been stripped of the sizing with acetone in an ultrasonic bath. A second batch of Nicalon fiber, with a bismaleimide compatible sizing (BMIC), was also tested.

Figure 1(a) presents a schematic illustrating the different types of surfaces that are present on a machined, continuous fiber reinforced composite. S1 denotes the resin rich surface that contacted the matched metal die mold surfaces. S2 is the surface produced by cutting the composite parallel to the fibers, and S3 is the surface that is produced by cutting the composite perpendicular to the fiber direction. Also shown (Figure 1(b)) is a micrograph of an aged composite that was cut parallel to the fiber direction. The inner core of the composite (the dark area) has not been oxidized. Surrounding this core on the top and bottom and left are layers of the composite that were degraded by a limited amount of oxidation (light area) controlled by diffusion of oxygen into the composite. The surfaces shown in this figure are referred to throughout this article.

3. FIBERS

Figure 2 shows scanning electron micrographs (SEM) of the circumferential surfaces of the four fibers. The surface features of the two ceramic fibers differed significantly from those of the graphite fibers. The ceramic

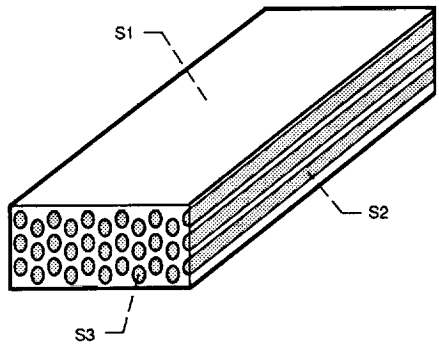

(a) Different types of surfaces.

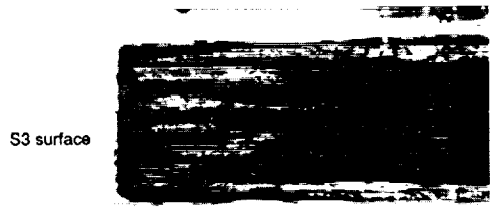

S1 surface

(b) Aged composite cross section showing degraded outer area. Inner dark area is undegraded.

Figure 1.— Composite surfaces.

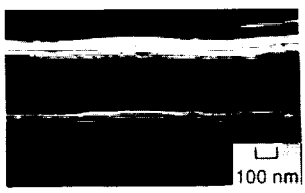

(a) Celion 6000.

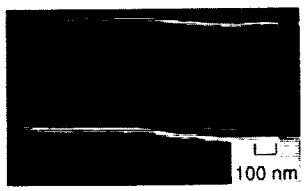

(b) T–40R.

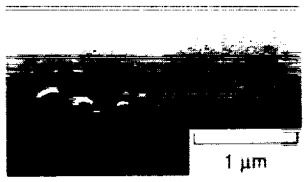

(c) Nicalon.

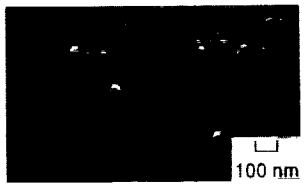

(d) Nextel 312.

Figure 2.—Surfaces of fibers that were studied.

fibers exhibited a topographically smoother but more grainy surface than the graphite fibers, with the Nextel 312 fibers having a much rougher surface than the Nicalon fibers. The graphite fibers (Figures 2(a) and 2(b)) have striations on the surfaces parallel to the fiber axes. The amount and size of the striations appear to be about the same for both the Celion 6000 and the T-40R fibers.

Surface areas, measured using Brunauer-Emmet-Teller isotherm analysis (BET) with Krypton as the gas, were 3.99 cm^2/mg and 5.5 cm^2/mg for the Celion 6000 and T-40R fibers respectively. Eckstein (9) measured values of 4.4 and 5.5 cm^2/mg for the same two fibers. Calculated surface areas, based on density and average diameter values, for the two fibers are 3.15 cm^2/mg for Celion 6000 and 2.26 cm^2/mg for the T-40R fiber.

The measured T-40R fiber surfaces are about 35 percent greater than those of the control reinforcement. However, because the T-40R fiber has a smaller diameter than the Celion 6000 fiber,it has about 37 percent more surface area per unit weight (or volume, since they both have the same density) than the Celion 6000 fiber.

Nicalon is a Si-C-O fiber that is derived from methylpolysilane (10). It contains 15 wt % oxygen. The surface is smooth and impervious (Figure 2(c)). A variety of surface connected porosity techniques, such as BET adsorption-desorption and mercury porosimetry, indicate that the measured surface area is close to the calculated area of 1.56 cm^2/mg (11). Calculations using rule-of-mixtures based on volume additivities for components in their appropriate states indicate that these fibers do contain about 16 percent porosity (12). Little or no open porosity is present, however. Therefore it is assumed that all the porosity is confined to the interior of the fiber.

The nominal fiber chemistry of the Nextel fiber is 62 percent Al_2O_3, 24 percent SiO_2, and 14 percent B_2O_3. A comparison of the measured density (2.7 to 2.9 g/cm^3) with the calculated density (3.36 g/cm^3) indicate a 17 percent void content. It is assumed that the voids are similar to those described for Nicalon fibers. From its appearance in Figure 2(d), The Nextel fiber possesses a rougher surface than the Nicalon reinforcement. The roughness is probably due to the size of the alumina crystallites. Normal sintering conditions for alumina lead to small grain size but also pore growth (13). Silica is added to the alumina to increase the crystallinity and crystallite size and also to decrease the porosity. A trade-off between crystallite size and porosity is apparently necessary. The cross section is oval rather than round as those of the other three fibers. The major diameter is twice the length of the minor diameter (13).

TABLE 1. - SURFACE CONCENTRATION OF ELEMENTS ON GRAPHITE AND CERAMIC FIBERS

Fiber	Carbon	Silicon	Al_2O_3	SiO_2	B_2O_3	Na	Ca	K	Fe
	Concentration, percent					Concentration, ppm			
Celion 6000	95.6	(a)	(a)	(a)	(a)	95	290	22	11
T-40R	98.9	(a)	(a)	(a)	(a)	4	7	1.2	(a)
Nicalon	28.4	55.5	(a)	---	(a)	600	200	(a)	300
Nextel 312	(a)	(a)	62	24	14	2100	200	10	50

[a]Not applicable.

TABLE 2. - FIBER PROPERTIES

Fiber	Tensile strength		Tensile modulus		Strain to failure, percent	Density, g/cm^3	Fiber diameter, μm
	MPa	ksi	GPa	Msi			
Celion 6000	3890	550	235.2	34	1.65	1.78	7.1
T-40R graphite	3640	528	296.5	43	1.23	1.81	5.1
Nicalon	2700	400	200	29	1.38	2.55	10-15
Nextel 312	1380-1724	200-250	151.7	22	0.91-1.14	2.7	10-12

The surface area is <2.0 cm^2/mg, which is the calculated geometric area (14).

The chemical composition, including some trace elements, are listed in Table 1 for the four fibers. The analyses were done using atomic spectra measurements of the bulk fiber.

4. MECHANICAL PROPERTIES

Table 2 contains a listing of the mechanical properties of the fibers that were used as reinforcements. The Nextel fiber possesses the lowest tensile strength, modulus, and strain-to-failure of the four reinforcements. This may be due to the grained texture of the surface (see Figure 2(d)) or high concentrations of a constituent in the grain boundaries. The grain boundaries may be considered to be surface defects that act as stress risers to cause failure below the normal strength value for the bulk material.

Table 3 presents the composite mechanical properties for laminates that are reinforced with the four fibers. Included in the table is a column with the heading "Flexural Strength (Rule of Mixtures)." The flexural strength is calculated in this column as 1.5 times the calculated rule-of-mixtures tensile strength of the composites (15). The effectiveness of translating fiber properties to composite properties is shown in the column entitled "Measured/Calculated." This is the measured value divided by the rule-of-mixtures value expressed in percentages. Except for the Celion 6000 and the Nicalon (BMIC) reinforced composites, the percent conversion is between 42 and 54 percent. The Celion 6000 reinforced composites, 90 percent, and the Nicalon(BMIC) reinforced composites, 90.8 percent, have much larger conversions. Table 3 also shows that the Nicalon (BMIC)

TABLE 3. - PMR-15 MATRIX COMPOSITE ROOM TEMPERATURE MECHANICAL PROPERTIES

Fiber[a]	Property									
	Flexural strength		Flexural strength (rule of mixtures)		$\left(\frac{\text{Measured}}{\text{Calculated}}\right)100$, percent	Flexural modulus		Interlaminar shear strength		Fiber volume, percent
	GPa	ksi	GPa	ksi		GPa	Msi	MPa	ksi	
Celion 6000 (U)	1.86	270.0	2.10	300.0	90.0	113.9	16.3	103.4	15.0	60.0
T-40R (U)	.88	128.0	2.02	294.1	43.5	75.0	10.9	75.0	10.9	55.7
Nicalon (S)	1.0	147.3	2.17	315.6	46.0	88.0	12.8	35.6	5.2	52.6
Nicalon (PVA)	.9	129.0	2.03	294.9	44.4	61.0	8.8	35.6	5.2	49.0
Nicalon (BMIC)	2.05	296.8	2.26	330.0	90.8	105.0	15.0	118.4	16.2	55.0
Nextel 312 (A-1100)	.05	72.5	1.02	147.6	48.5	28.5	4.1	45.8	6.6	49.2

[a]Unsized, U; stripped of sizing with acetone, S; sized with polyvinyl acetate, PVA; bismaleimide-compatible sizing, BMIC; A-1100 sizing, A-1100.

reinforcement imparted the greatest flexural strength and interlaminar shear strength (ILSS) to the processed composites.

5. AIR AGING BEHAVIOR

5.1 Graphite Fibers The composites that were studied differed significantly in air aging behavior. It is quite interesting that major differences in the effects of high temperature exposure to air even exist between the two graphite fibers. These differences are presented in this section.

The relationship between weight loss and aging time at 316°C for the two bare graphite fibers at are shown in Figure 3. It is evident that the T-40R fiber is much more thermally stable than the Celion 6000 fiber. Data for the bare ceramic fiber are not included in this figure since, naturally, the fibers exhibit no significant weight changes, except for sizing deterioration, under these conditions.

The 316 °C air aging weight loss history for aging times less than 1000 hr is shown for each of the six PMR-15 composites in Figure 4. The thermo-oxidative stability of the fibers is not reflected in composite stability. The least thermally stable fiber, the Celion 6000 fiber, produced the most thermally stable composite. The most thermally stable ceramic fibers did not impart their stability to the PMR-15 composites. They were the least stable composites.

The geometry of the Celion 6000/PMR-15 composites substantially affects the rate of weight loss (5-6). The geometric effects were found to be due to excessive weight loss from the cut specimen edges, especially the S3

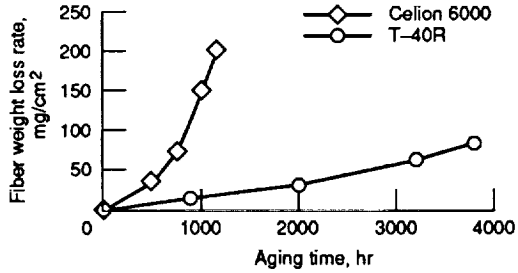

Figure 3.— Weight loss rate of graphite fibers aging in air at 316 °C.

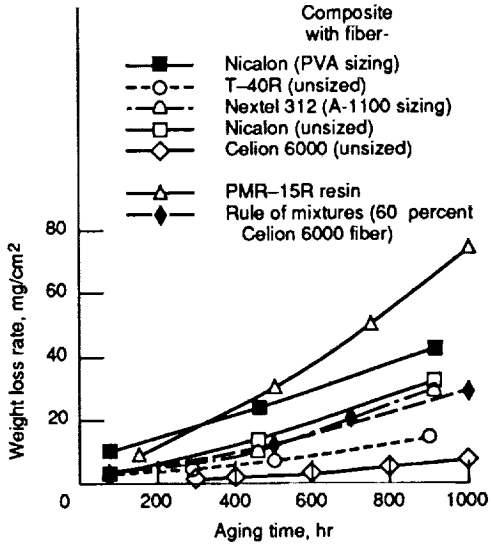

Figure 4.—Weight loss rate of PMR-15 composites aging in air at 316 C.

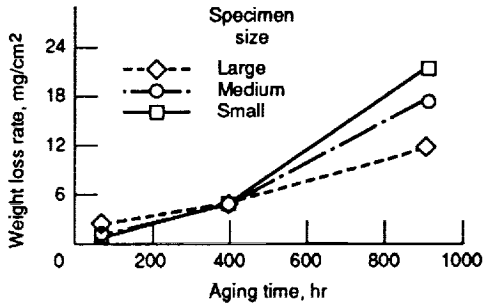

Figure 5.—Weight loss rate of T–40R-fiber-reinforced PMR–15 composites aged in air at 316 °C.

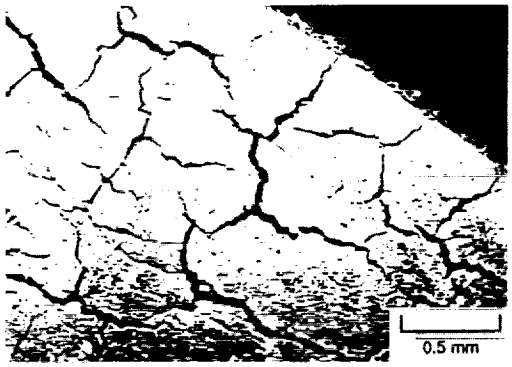

(a) Celion 6000/PMR–15 composite after 1212 hours.

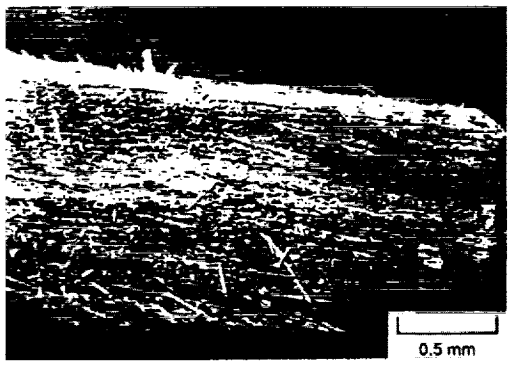

(b) T–40R/PMR–15 composite after 889 hours.

Figure 6.—End views (S3 surface) of graphite-fiber-reinforced PMR–15 composites after aging in air at 316 °C.

(a) Celion 6000.

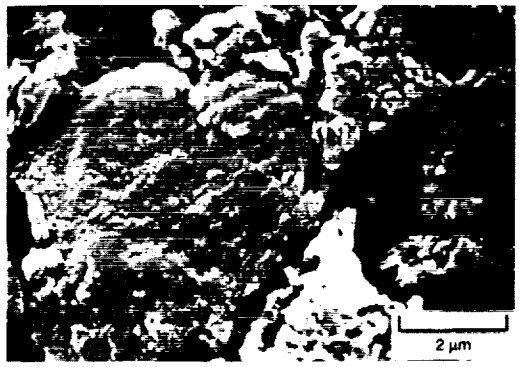

(b) T–40.

Figure 7.—End views (S3 surface) of graphite-fiber-reinforced PMR–15 composites after aging in air at 316 °C—greater magnifications of views shown in figure 8.

surfaces. The edge effects were enhanced by the development of cracks in the edges. The cracks developed in the S3 surfaces and increased as the aging time progressed. The damage is shown in Figure 5(a). The T-40R fiber reinforced composites showed no geometry effects initially, but after about 400 hr, geometry effects became apparent (7). They showed no signs of cracks, however. (See Figure 6) The ceramic fiber reinforced composites showed no geometry effects at all (7). Cracks were observed in the S3 surfaces in this study.

Larger magnifications of Figure 5 are shown in Figure 7. Figure 7(a) shows the end view (surface S3) of a Celion 6000 fiber in a PMR-15 composite. The

fiber end exhibits a very erosive-like surface, one with edges that appear to be worn smooth. The fiber cracked into distinct, separate pieces. Although the fiber circumferential surfaces were protected from oxidation by the matrix during air aging, the end cracking allows increased access to the inner part of the composite.

It should be noted that degradation of the fiber-matrix interface is also apparent in Figure 7(a) as evidenced by the existence if a space between the matrix and the fiber. Fiber diameter measurements from SEM micrographs indicate that the fiber is degrading, resulting in a reduction in the fiber diameter. The diameter of the resultant hole in the matrix remains the same as the initial fiber diameter.

The typical appearance of air aged fibers, along the S2 surface at a location away from the fiber ends (S3 surface), is shown in Figure 8. Deep striations develop along the surface and parallel to the fiber axis. These striations are much more pronounced than those on the surface of the Celion 6000 shown in Figure 2(a).

Even the surfaces of the fibers that are in parts of the composite that are not directly exposed to the air undergo changes from the thermal exposure alone. Figures 9(a) and 9(b) show the surfaces of a fiber end and a fiber circumferential surface that are located in the degraded outer layer shown in Figure 1(b). It appears in both cases that there is a coating over the normally smooth fiber surfaces. The texture of the surfaces resemble that of an ear of corn. When the composite was digested to measure the fiber fraction, or when the surface is exposed to air at an elevated temperature, this surface texture disappeared leaving the normal surface shown in Figure 8. These figures suggest that a reaction product forms at the fiber-matrix interface at 316 °C under anaerobic conditions and the reaction products disappear when exposed to oxidizing conditions. One item of interest in Figure 7(a) is that the fiber appears to be made up of small fibrils of about 0.4 μm in diameter.

Figure 7(b) shows the end of a T-40R fiber that has been exposed to 316 °C air at the cut S3 surface of a PMR-15 composite. The matrix surface has receded leaving the T-40R fibers exposed like whiskers. The surface of the cut fiber looks as if it has the texture of ground meat. In contrast to the Celion 6000 fiber ends shown in Figure 7(a), the corners are not rounded and the surface contours are not smoothed out.

Focusing on the matrix in Figure 10, it is apparent that there is preferential oxidative attack in the matrix. The fibers are surrounded by what looks like relatively less aggressively oxidized layers of matrix

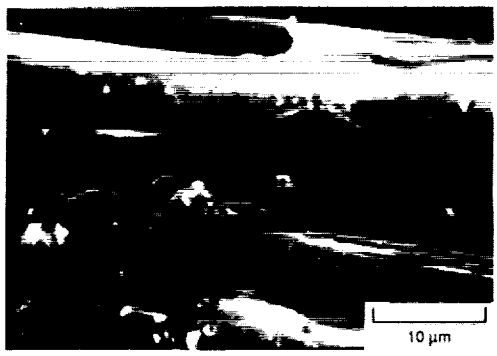

Figure 8.— Scanning electron micrograph of Celion 6000 fiber (S2 surface) after air aging in a PMR–15 composite.

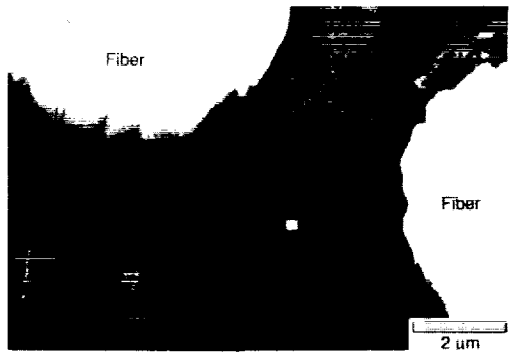

Figure 10.—End views (S3 surface) of T–40R/PMR–15 composite aged in air at 316°, showing selective oxidation of matrix.

(a) Fiber ends (S3 surface).

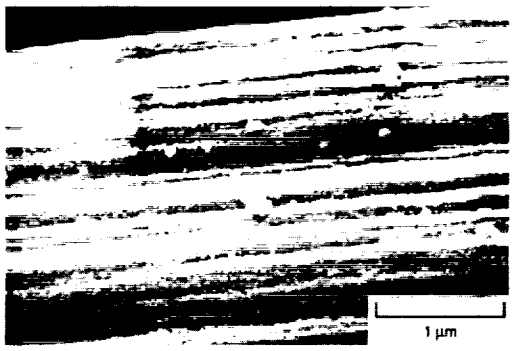

(b) Fiber circumferential surface (S2 surface).

Figure 9.— Celion 6000/PMR–15 composite aged in air at 316 °C. Fibers are from degraded outer layer but have not been directly exposed to air.

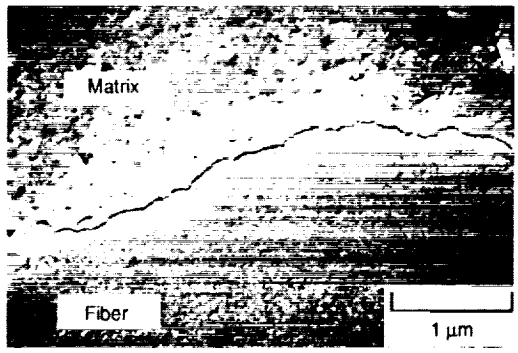

(a) Crack at interface.

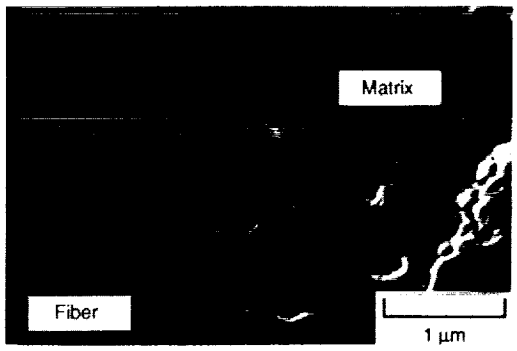

(b) Voids at interface.

Figure 11.—T–40R composite interior material aged in air at 316 °C.

material, measured to be 1.5 μm in thickness, which form cylindrical sheaths around the fibers. The matrix material outside of these sheaths and between them, with a tricuspid shape, appears to be more aggressively attacked by the air than the sheaths. The penetration is deeper and the material has a spongy, void dominated appearance. It also appears that there are separations between the fibers and the matrix.

In order to look more closely into the origin of the voids in the matrix outside of the sheath material that surrounds the T-40R fibers in Figure 10, air-aged specimens of T-40R/PMR-15 composites were cut to expose their interiors. The specimen interiors were protected from direct contact with the environment. The two scanning electron micrographs of the specimen in Figure 11 show T-40R graphite fibers surrounded by the PMR-15 matrix. The specimen was mounted in a metallographic mount and polished. Very small voids are visible, but there are no signs of matrix differences that would indicate the presence of sheaths around the fibers. One item of significance is the presence of a separating crack or the concentration of voids at the interface in the micrographs. Also notice how flat the fiber surfaces are from the polishing.

For purposes of comparison with the T-40R fiber reinforced composite shown in Figure 11, the same type of polished specimen was prepared from a Celion 6000 reinforced composite specimen. The fiber surface and the matrix surface, as shown in Figure 12, appear different from the T-40R fiber and matrix shown in Figure 11. The matrix exhibits more grainy features and the fiber surface contains a significant amount of relief with small hills and valleys in evidence. It is noteworthy to mention that there is no visible separation between the fiber and the matrix.

5.2 CERAMIC FIBERS The difference between the oxidation of composites reinforced with ceramic fibers and those reinforced with graphite fibers is illustrated in Figure 13 which shows the S3 surfaces of the Nicalon and Nextel composites. The oxidation attack is concentrated in the matrix, but there was no preferential oxidative attack like that on the T-40R composite. Figure 13 shows significant separations between the PMR-15 matrix and the Nicalon and Nextel fibers. The width of the separations is estimated to be about 0.5 μm.

The extent of interfacial bonding between the ceramic fiber and the polyamide matrix is illustrated in Figure 14 which shows the fiber surfaces of a composite specimen that was cleaved parallel to the fibers. Note that

Figure 12.—Central portion of aged Celion 6000/PMR–15 composite specimen aged in air at 316 °C.

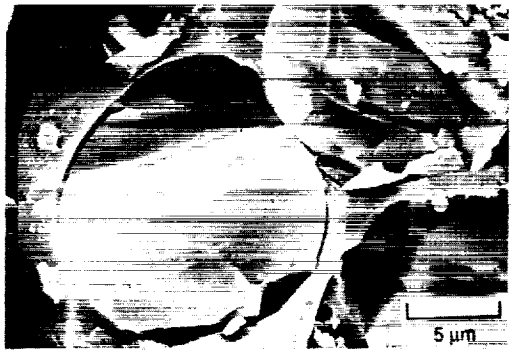

(a) Nicalon.

(b) Nextel 312.

Figure 13.—End views (S3 surfaces) of ceramic composites aged in air at 316°C, showing separations between fibers and matrix.

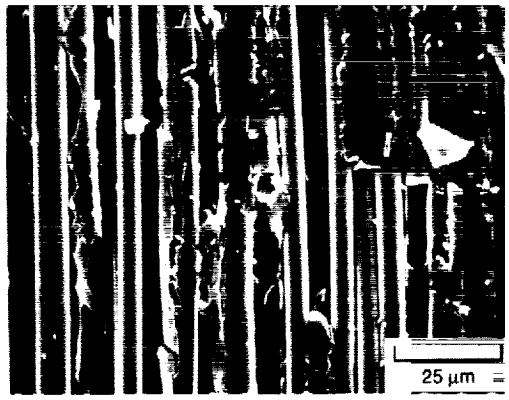

Figure 14.—Interior surface (S2 surface) of Nicalon composite produced by cleaving with a razor. No signs of good fiber-to-matrix bonding are visible. Fiber surfaces are clean.

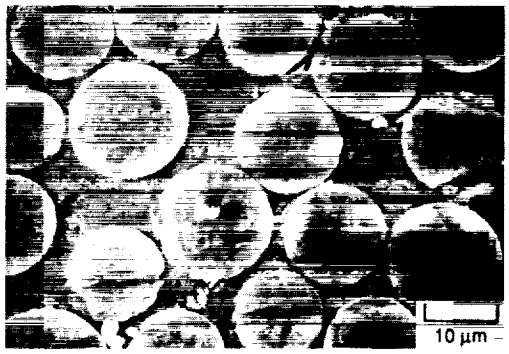

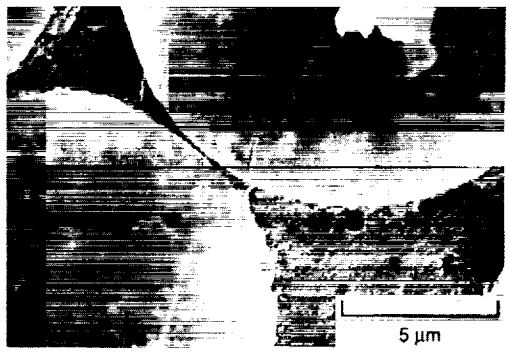

Figure 15.—Interior of Nicalon/PMR–15 composite aged in air at 316 °C. No fiber-matrix separations are visible.

no particles of the matrix are attached to the fiber surfaces. This indicates poor bonding at the interface all along the fibers and not just at the S3 surfaces as shown in Figure 13.

Figure 15 shows the interior of a ceramic composite and is a typical micrograph of the interfacial features of all of the ceramic/PMR-15 composites that were studied including the BMIC Nicalon reinforced composite. There is no evidence of matrix oxidation along the interface in

the interior of the composites. All the weight loss appears to be confined to the exterior surfaces of the ceramic fiber reinforced composites.

6. DISCUSSION

One of the most important conclusions gleaned from the studies done at the Lewis Research Center is that the thermal stability of the fibers is not the dominant factor in determining composite stability. The reason for this is that the fiber/matrix interface plays such an important role in both the thermal and mechanical behavior of polymer matrix composites.

The substantial difference between the mechanical properties of composites with each of the two graphite fibers as reinforcing material is probably due to the degree of observed bonding between the fibers and the polyamide matrix. In Figure 12 the bond between the Celion 6000 and the PMR-15 is very tight. On the other hand, due to fiber/matrix separations in Figure 11, the T-40/PMR-15 interfacial bond appears to be less tight. Although the T-40R fiber has a slightly rougher surface and a larger surface area per unit weight than the Celion 6000 fiber, the transfer of loads from the fiber to the resin matrix was more efficient for the Celion 6000 fiber. So, for this case, surface area differences and the resultant proposed mechanical bonding differences were not a significant factor in influencing composite mechanical properties. One may reasonably speculate that the superior properties of the Celion 6000 composite are due to chemical bond interactions between the fiber and the matrix.

Except for the BMIC sized Nicalon reinforced composite, the inadequate bonding that caused the ceramic fibers to have low mechanical properties was probably due to the lack of a suitable sizing that could sustain the processing temperature of 316 °C as well as the fiber surface, which was significantly smoother than the surfaces of the graphite fibers. The BMIC sized Nicalon reinforced composite exhibited superior room temperature mechanical properties, probably because the sizing withstood the processing temperature for the required time and promoted a good interfacial bond. The results of the thermal aging tests indicate that this bonding broke down after extended periods at 316 °C since the weight loss rate did not differ significantly from those of the other Nicalon composites.

The information provided by Figures 7, 11, and 12 indicate that the two graphite fibers have different structures. The contrast between Figures 11 and 12 indicate that the T-40R fiber (Figure 11) may have a more uniform structure and therefore a more evenly polished surface than that of the Celion 6000 fiber (Figure 12). The surface relief shown in the latter figure appears to be a less severe condition than that of the oxidized

Celion 6000 fiber shown in Figure 8, but one that can be imagined to be the onset of a transformation into a final appearance similar to it.

The following hypothesis can be made from the visible evidence of bonding between the two constituents of the graphite composite constituents. The more rapid oxidation of the fibers in the Celion 6000 reinforced composite causes the fibers to recede into the composite, and the stored strain energy in the matrix may result in matrix cracking along the S3 surfaces. In contrast the strained matrix in the T-40R reinforced composite is oxidized away leaving only exposed fibers with no matrix cracking. One can consider that the S3 surface appearance depends on both the degree of bonding between the fiber and the matrix and on the relative thermal stability of the resin and the fiber.

The ceramic fiber reinforced composites, that were studied, appear to have oxidized at the S3 surfaces, in general, by a mechanism similar to that experienced by the T-40R graphite composites. Rather than a selective oxidation in the fiber or the matrix, the composite degradations appear to take place at the ceramic-polymer interfaces as shown by the interfacial gaps in Figures 12 and 13. Because these gaps did not extend for a significant distance into the composites, they could not have been caused by unequal shrinkage of the composite constituents during cool down after curing. Figure 15 shows a cross section of the interior of an aged ceramic fiber reinforced composite.

7. CONCLUSIONS

The following conclusions were made from the results of this study:

1. Fiber thermal stability is not translated into composite stability.

2. Bonding forces are more important than fiber surface area and topography in establishing fiber-matrix bond efficiency.

3. Ceramic fibers and thermally stable graphite fibers may require high temperature sizing to promote sufficient interfacial bonding to provide good mechanical properties and thermal stability to their composites. However, light metal concentrations at the fiber-matrix interface, from sizings or the fibers themselves, could enhance oxidation in this area.

8. ITEMS FOR FUTURE STUDY

The following observations were made during this study and efforts should be made to verify them and to investigate them further:

1. Celion 6000 fibers and PMR-15 polyamide may react at their interface during exposure to thermal aging.

2. The carbon structure in the Celion 6000 fiber appears to change during aging. The fiber seems to transform into a nonhomogeneous material with varying degrees of hardness across the diametral cross section.

3. The effect of stresses on the thermal behavior of polymers may be significant.

4. Oxidation mechanisms may generate thermal stress gradients that can cause composite cracking and enhanced oxidation which would be significantly influenced by geometry factors.

9. REFERENCES

1. Hanson, M.P.; and Serafini, T.T.: Effects of Thermal and Environmental Exposure on the Mechanical Properties of Graphite/Polyamide Composites. Space Shuttle Materials, SAMPE, 1971, pp. 31-38. (Also, NASA TM X-67893.)
2. Gibbs, H.H.; Wendt, R.C.; and Wilson, F.C.: Carbon Fiber Structure and Stability Studies. Proceedings of the 33rd Annual Conference, Reinforced Plastics/Composites Institute, The Society of Plastics Industry, 1978, pp. 24F1-24F9.
3. Eckstein, B.H.: Oxidation of Carbon Fibres in Air Between 230° and 375 °C. Fibre Sci. Technol., vol. 14, no. 2, Feb. 1981, pp. 139-156.
4. Scola, D.A.: Thermo-Oxidative Stability of Graphite Fiber/PMR-15 Polyamide Composites at 350 °C. High Temperature Polymer Matrix Composites, NASA CP-2385, 1985, pp. 217-242.
5. Bowles, K.J.; and Meyers, A.E.: Specimen Geometry Effects on Graphite/PMR-15 Composites During Thermo-Oxidative Aging. Material Sciences for the Future, J.L. Bauer and R. Dunaetz, eds., SAMPE, 1986, pp. 1285-1299. (Also, NASA TM-87204.)
6. Bowles, K.J.; and Nowak, G.: Thermo-Oxidative Stability Studies of Celion 6000/PMR-15 Unidirectional Composites, PMR-15, and Celion 6000 Fiber. J. Compos. Mater., vol. 22, no. 10, Oct. 1988, pp. 966-985.
7. Bowles, K.J.: Thermo-Oxidative Stability Studies of PMR-15 Polymer Matrix Composites Reinforced With Various Continuous Fibers. Advanced Materials: The Challenge for the Next Decade, Book 1, G. Janicki, V. Bailey, and H. Schjelderup, eds. SAMPE, 1990, pp. 147-161.
8. Vannucci, R.D.: PMR-15 Polyamide Modifications for Improved Prepreg Tack. Proceedings of the 1982 National Technical Conference: The Plastic's ABC's, Society of Plastics Engineers, 1982, pp. 131-133. (Also, NASA TM-82951.)

9. Eckstein, B.H.: The Weight Loss of Carbon Fibers in Circulating Air. Material Sciences For The Future, 18th International SAMPE Technical Conference Proceedings, J.L. Bauer and R. Dunaetz, eds., SAMPE, 1986, pp. 149-160.

10. Nairn, J.A.: Thermoelastic Analysis of Residual Stresses in Unidirectional, High Performance Composites. Polymer Composites, vol. 6, no. 2, pp. 123-130.

11. Bowles, K.J.: A Thermally Modified Polymer Matrix Composite Material With Structural Integrity to 371 °C. Materials-Processes: The Intercept Point, International SAMPE Technical Conference Series, Vol. 20, 1988, pp. 552-561. (Also, NASS TM-100922.)

12. Lipowitz, J.; Rabe, J.A.; Frevel, L.K; and Miller, R.L.: Characterization of Nanoporosity in Polymer-Derived Ceramic Fibers by X-Ray Scattering Techniques. J. Mater. Sci., vol. 25, no. 4, Apr. 1990, pp. 2118-2124.

13. Holtz, A.R.; and Grether, M.F.: High Temperature Properties of Three Nextel Ceramic Fibers. Advanced Materials Technology '87, 32nd International SAMPE Symposium and Exhibition, Vol. 32, SAMPE, 1987, pp. 245-256.

14. Watt, W.; and Perov, B.V.: Strong Fibres. Elsevier Science Publishers, 1985, pp. 124-130.

15. Lubin, G., ed.: Handbook of Composites. Van Nostrand Reinhold Co., 1982, pp. 196-209.

NASA
National Aeronautics and Space Administration

Report Documentation Page

1. Report No.	2. Government Accession No.	3. Recipient's Catalog No.
NASA TM-104416		

4. Title and Subtitle	5. Report Date
A Comparison of Fiber Effects on Polymer Matrix Composite Oxidation	
	6. Performing Organization Code

7. Author(s)	8. Performing Organization Report No.
Kenneth J. Bowles	E-6248
	10. Work Unit No. 510-01-50

9. Performing Organization Name and Address	11. Contract or Grant No.
National Aeronautics and Space Administration Lewis Research Center Cleveland, Ohio 44135-3191	
	13. Type of Report and Period Covered: Technical Memorandum

12. Sponsoring Agency Name and Address	14. Sponsoring Agency Code
National Aeronautics and Space Administration Washington, D.C. 20546-0001	

15. Supplementary Notes

Prepared for the Second Japan International Symposium and Exhibition sponsored by the Society for the Advancement of Materials and Process Engineering, Chiba, Japan, December 11-14, 1991. Responsible person, Kenneth J. Bowles, (216) 433-3201.

16. Abstract

A number of thermo-oxidative stability studies addressing the effects of fiber reinforcement on composite thermal stability and the influence of geometry on the results of aging studies have been performed at the Lewis Research Center. The information presented herein, a compilation of some results from these studies, shows the influence of the reinforcement fibers on the oxidative degradation of various PMR-15 composites. Reinforcement of graphite and ceramics were studied and three composite oxidation mechanisms were observed. One was a dominant attack of the reinforcement fiber, the second was the aggressive oxidation of the matrix material, and the third was interfacial degradation.

17. Key Words (Suggested by Author(s))	18. Distribution Statement
Polyimides; Composite materials; Graphite; Fibers; Ceramic fibers; Oxidation	Unclassified - Unlimited Subject Category 24

19. Security Classif. (of the report)	20. Security Classif. (of this page)	21. No. of pages	22. Price*
Unclassified	Unclassified	18	A03

NASA FORM 1626 OCT 86

*For sale by the National Technical Information Service, Springfield, Virginia 22161